Quantum Information and Computation, Vol. , No. (20) 000–000

THREE-PARTY ENTANGLEMENT IN TRIPARTITE TELEPORTATION SCHEME THROUGH NOISY CHANNELS

EYLEE JUNG
Department of Physics, Kyungnam University, Kyungsangnam do, Masan, 449 Wolyoung Dong, 631-701, Korea

MI-RA HWANG
Department of Physics, Kyungnam University, Kyungsangnam do, Masan, 449 Wolyoung Dong, 631-701, Korea

DAEKIL PARK
Department of Physics, Kyungnam University, Kyungsangnam do, Masan, 449 Wolyoung Dong, 631-701, Korea

SAYATNOVA TAMARYAN
Theory department, Yerevan Physics Institute, 2 Alikhanian Br., Yerevan, 375036, Armenia

Received (received date)
Revised (revised date)

In this paper we have tried to interpret the physical role of three-tangle and π-tangle in real physical information processes. For the model calculation we adopt the tripartite teleportation scheme through various noisy channels. The three parties consist of sender, accomplice and receiver. It is shown that the π-tangles for the X- and Z-noisy channels vanish at the limit $\kappa t \to \infty$, where κt is a decoherence parameter introduced in the master equation in the Lindblad form. At this limit the maximum fidelity of the receiver's state reduces to the classical limit 2/3. However, this nice feature is not maintained for the Y- and isotropy-noise channels. For the Y-noise channel the π-tangle vanishes when $0.61 \leq \kappa t$. At $\kappa t = 0.61$ the maximum fidelity becomes 0.57, which is much less than the classical limit. Similar phenomenon occurs for the isotropic noise channel. We also compute analytically the three-tangles for the X- and Z-noise channels. The remarkable fact is that the three-tangle for the Z-noise channel coincides exactly with the corresponding π-tangle. In the X-noise channel the three-tangle vanishes when $0.10 \leq \kappa t$. At $\kappa t = 0.10$ the fidelity of the receiver's state can reduce to the classical limit provided that the accomplice performs the measurement appropriately. However, the maximum fidelity becomes 8/9, which is much larger than the classical limit. Since the Y- and isotropy-noise channels are rank-8 mixed states, their three-tangles are not computed explicitly in this paper. Instead, their upper bounds are derived by making use of the analytic formulas of the three-tangle for other noisy channels. Our analysis strongly suggests that different tripartite entanglement measure is needed whose value is between three-tangle and π-tangle.

Keywords: entanglement measures, quantum decoherence, Quantum teleportation

Communicated by: to be filled by the Editorial

1. Introduction

It is well-known that quantum entanglement is a valuable physical resource in quantum information theories [1]. Among the best known applications of entanglement are quantum state teleportation [2] and superdense coding [3]. Furthermore, entanglement is responsible for the speed-up of the quantum computer [4]. In this reason there has been a flurry of activity recently in the research of entanglement.

Many new properties for the entanglement of three- or higher-qubit pure states have been reported in the recent papers [5]. However, it is in general more difficult to understand the properties of entanglement for mixed states except the bipartite case[a]. These difficulties we are about to discuss originate from the fact that the mixed state entanglement is defined by a convex-roof extension [6, 7] of the pure state entanglement. Therefore, in order to compute the entanglement defined by convex-roof method one should derive the optimal decomposition for a given mixed state. Generally, however, it is a non-trivial task to derive the optimal decomposition for arbitrary mixed states. This computational difficulty makes it hard to characterize the multipartite entanglement for mixed states.

For two-qubit states, fortunately, Wootters found how to derive the optimal decomposition for the concurrence, one of the entanglement measure for bipartite states, in Ref.[8, 9]. Thus, one can compute the concurrence $\mathcal{C}(\rho)$ for arbitrary mixed states ρ by Wootters formula

$$\mathcal{C}(\rho) = \max(0, \lambda_1 - \lambda_2 - \lambda_3 - \lambda_4), \tag{1}$$

where λ_i's are the eigenvalues, in decreasing order, of the Hermitian matrix

$$\sqrt{\sqrt{\rho}(\sigma_y \otimes \sigma_y)\rho^*(\sigma_y \otimes \sigma_y)\sqrt{\rho}}.$$

One of the most fundamental properties of entanglement is monogamy. For three qubits the trade-off is described by Coffman-Kundu-Wootters(CKW) monogamy inequality [10]

$$\mathcal{C}^2_{AB} + \mathcal{C}^2_{AC} \leq \mathcal{C}^2_{A(BC)}, \tag{2}$$

where $\mathcal{C}_{AB}$ and $\mathcal{C}_{AC}$ are concurrences for the reduced states $\rho^{AB} = \mathrm{Tr}_C|\psi_{ABC}\rangle\langle\psi_{ABC}|$ and $\rho^{AC} = \mathrm{Tr}_B|\psi_{ABC}\rangle\langle\psi_{ABC}|$, and $\mathcal{C}_{A(BC)}$ is a concurrence between a pair BC and A. Therefore, $\mathcal{C}_{A(BC)}$ represents the total entanglement of the qubit A arising due to the remaining qubits. For pure states $\mathcal{C}^2_{A(BC)}$ reduces to $4\mathrm{det}\rho^A$, where $\rho^A = \mathrm{Tr}_{BC}|\psi_{ABC}\rangle\langle\psi_{ABC}|$, and is called one-tangle. In this sense, the inequality (2) indicates that the total one-tangle is greater than sum of two-tangles.

This monogamy implies that the quantity $\tau_{ABC} \equiv \mathcal{C}^2_{A(BC)} - (\mathcal{C}^2_{AB} + \mathcal{C}^2_{AC})$, known as residual entanglement or three-tangle, represents true three-particle entanglement. For the three-qubit pure state $|\psi\rangle = \sum_{i,j,k=0}^{1} a_{ijk}|ijk\rangle$ the three-tangle τ_{ABC} becomes[10]

$$\tau_{ABC} = 4|d_1 - 2d_2 + 4d_3|, \tag{3}$$

where

$$\begin{aligned} d_1 &= a^2_{000}a^2_{111} + a^2_{001}a^2_{110} + a^2_{010}a^2_{101} + a^2_{100}a^2_{011}, \\ d_2 &= a_{000}a_{111}a_{011}a_{100} + a_{000}a_{111}a_{101}a_{010} + a_{000}a_{111}a_{110}a_{001} \\ &\quad + a_{011}a_{100}a_{101}a_{010} + a_{011}a_{100}a_{110}a_{001} + a_{101}a_{010}a_{110}a_{001}, \\ d_3 &= a_{000}a_{110}a_{101}a_{011} + a_{111}a_{001}a_{010}a_{100}. \end{aligned} \tag{4}$$

[a]Even for bipartite case still we do not know how to compute the concurrence of the arbitrary mixed states in the qudit system except qubit case.

The three-tangle defined by Eq.(3) coincides exactly with the modulus of a Cayley's hyperdeterminant[11, 12] and is an invariant quantity under the local $SL(2,C)$ transformation[13, 14].

The three-tangle (3) has following two important properties. Firstly, for a completely separable ($A-B-C$) and biseparable ($A-BC$, $B-AC$, $AB-C$) states τ_{ABC} becomes zero. This means that the three-tangle quantifies truly tripartite entanglement contained in a pure three-qubit state. Secondly, the three-tangle is identically zero for the W class states and strictly positive for the Greenberger-Horne-Zeilinger(GHZ) class states, where a classification is introduced by Dür, Vidal and Cirac [15]. In particular, for the GHZ [16]

$$|GHZ\rangle = \frac{1}{\sqrt{2}}\left(|000\rangle + |111\rangle\right) \tag{5}$$

and W [15]

$$|W\rangle = \frac{1}{\sqrt{3}}\left(|001\rangle + |010\rangle + |100\rangle\right) \tag{6}$$

states the three-tangles become

$$\tau_{ABC}(|GHZ\rangle) = 1 \qquad \tau_{ABC}(|W\rangle) = 0. \tag{7}$$

The whole set of three-qubit pure states can be divided into subsets of completely separable, biseparable, GHZ-type, and W-type states through stochastic local operation and classical communication(SLOCC). The subset of GHZ states is an open set whiles other subsets are compact. It is shown that GHZ is the only class of three-qubit states which are not determined by their two-partite marginals [17] and arbitrary W states are uniquely determined by their two-party reduced density matrices [18]. That is, GHZ states possess a genuine tripartite entanglement and W states possess a genuine two partite entanglement. The three-tangle is positive on the open subset of GHZ states and decreases monotonically as approaching to the boundary of the open subset. Eventually it vanishes at the compact subset of W class. Thus, the three-tangle quantifies genuine tripartite, i.e. GHZ-type, entanglement of a three qubit state, but does not detect W-type entanglement at all [19].

For mixed states the three-tangle is defined by a convex-roof method[6, 7] as follows:

$$\tau_{ABC}(\rho) = \min \sum_i p_i \tau_{ABC}(\rho_i), \tag{8}$$

where the minimum is taken over all possible ensembles of pure states. The pure state ensemble corresponding to the minimum τ_{ABC} is called optimal decomposition. It is in general difficult to derive the optimal decomposition for arbitrary mixed states. Fortunately, Lohmayer *et al* [20] have derived recently the optimal decomposition for the mixed state ρ of the following form

$$\rho(p) = p|GHZ\rangle\langle GHZ| + (1-p)|W\rangle\langle W| \tag{9}$$

and computed explicitly the three-tangle. They also have found that the CKW inequality (2) holds for mixed states(as well as for pure states). Subsequently, the three-tangle for the rank-2 mixed state composed of the generalized GHZ and generalized W states has been computed in Ref.[21]. Furthermore, in Ref.[22] the optimal decompositions and the three-tangle for the

rank-3 mixed state composed of GHZ, W, and flipped W states have been derived explicitly. Most recently, the three-tangle for the rank-4 mixed states composed of 4-different GHZ states has been computed explicitly in Ref.[23].

On the other hand, in order to detect the three-party entanglement of W states we need to use a new three-party entanglement measure different from the three-tangle. One of the candidates is a π-tangle discussed in Ref.[24]. The π-tangle is defined in terms of the global negativities [25]. For a three-qubit state ρ they are given by

$$\mathcal{N}^A = ||\rho^{T_A}|| - 1, \qquad \mathcal{N}^B = ||\rho^{T_B}|| - 1, \qquad \mathcal{N}^C = ||\rho^{T_C}|| - 1, \tag{10}$$

where $||R|| = \mathrm{Tr}\sqrt{RR^\dagger}$, and the superscripts T_A, T_B and T_C represent the partial transposes of ρ with respect to the qubits A, B and C respectively. Using the separability criterion based on partial transpose [26, 27, 28] it is easy to show that the global negativities vanish for separable states. It is worthwhile noting that the computation of the global negativities is relatively simple compared to the concurrence or three-tangle for mixed states since it does not need the convex-roof extension. In addition, the negativities also satisfy the monogamy inequality

$$\mathcal{N}^2_{AB} + \mathcal{N}^2_{AC} \leq \mathcal{N}^2_{A(BC)} \tag{11}$$

like concurrence. Then, the π-tangle is defined as

$$\pi_{ABC} = \frac{1}{3}(\pi_A + \pi_B + \pi_C), \tag{12}$$

where

$$\pi_A = \mathcal{N}^2_{A(BC)} - (\mathcal{N}^2_{AB} + \mathcal{N}^2_{AC}) \quad \pi_B = \mathcal{N}^2_{B(AC)} - (\mathcal{N}^2_{AB} + \mathcal{N}^2_{BC}) \quad \pi_C = \mathcal{N}^2_{(AB)C} - (\mathcal{N}^2_{AC} + \mathcal{N}^2_{BC}). \tag{13}$$

It is easy to show that the π-tangles for $|GHZ\rangle$ and $|W\rangle$ become

$$\pi_{ABC}(|GHZ\rangle) = 1 \qquad \pi_{ABC}(|W\rangle) = \frac{4}{9}(\sqrt{5} - 1) \sim 0.55. \tag{14}$$

Thus the π-tangle detects W-like(as well as GHZ-like) entanglement.

In this paper we would like to explore the physical role of the tripartite entanglement in the real quantum information process. In order to discuss this issue we adopt the tripartite teleportation scheme discussed in Ref.[29]. Similar issue was discussed in Ref.[30], where the physical role of the concurrence is discussed in the bipartite teleportation through noisy channels. Ref.[30] has shown that the concurrences of the mixed state quantum channels arising due to some noises vanish in the region of $\bar{F} \leq 2/3$, where $\bar{F}$ is an average fidelity between initial Alice's unknown state and final Bob's state. Since $\bar{F} = 2/3$ corresponds to the best possible score when Alice and Bob communicate with each other through the classical channel[31], this result indicates that the entanglement of the quantum channel is a genuine physical resource for the teleportation process.

This paper is organized as follows. In section II we re-formulate the tripartite teleportation process[29] in terms of density matrices. This re-description allows us to formulate the tripartite teleportation process when quantum channel is a mixed state. Several basic quantities are calculated in this section, which are essential for the calculation of various fidelities in

next sections. In section III we compute the various fidelities when the tripartite teleportation process is performed through noisy channels. In section IV we compute the π-tangles for the various noisy channels. It is shown that the π-tangles for all noise channels decrease with increasing the decoherence parameter κt. This is in fact expected due to the fact that the decoherence in general disentangles quantum states like "sudden death". The π-tangle for the X- and Z-noise channels vanish at the limit $\kappa t \to \infty$. However, the π-tangles for the Y- and isotropy-noise channels are found to be non-zero at the finite range of the decoherence parameter κt. In section V we compute the three-tangles for the X- and Z-noise channels. It is shown that the three-tangle for the Z-noise channel is exactly the same as the corresponding π-tangle. The three-tangle for the X-noise channel is shown to have three different expressions depending on the range of κt. Since the channels for the Y- and isotropy-noises are rank-8 mixed states, there is no general method to compute the three-tangles in these cases so far. However, we will derive the upper bound of these three-tangles. In section VI we analyze the π-tangle and three-tangle by making use of the fidelity between sender's unknown state and receiver's final state. The π-tangle seems to be too large to have a nice physical interpretation. The three-tangle also seems to be too small. This analysis strongly suggests that we may need a different tripartite entanglement measure whose value is between three-tangle and π-tangle.

2. Basic Quantities

In this section we want to re-formulate the tripartite teleportation scheme in terms of the density matrices[32]. It involves sender (Alice), accomplice (Bob) and receiver (Charlie). Initially, they share each single qubit of the GHZ state, *i.e.* $\rho_{GHZ} = |GHZ\rangle_{234}\langle GHZ|$. The purpose of the tripartite teleportation is as follows. Firstly, Alice at location 2 wants to transport a single qubit state

$$\rho_{in} = |\psi_{in}\rangle\langle\psi_{in}| \qquad |\psi_{in}\rangle = \cos\left(\frac{\theta}{2}\right) e^{i\phi/2}|0\rangle + \sin\left(\frac{\theta}{2}\right) e^{-i\phi/2}|1\rangle \tag{15}$$

to the receiver, Charlie, at location 4 with fidelity $\bar{F}_C$ as high as possible with a help of the accomplice, Bob, at location 3. At the same time Alice wants to transport ρ_{in} to the accomplice, Bob, with fidelity $\bar{F}_B$ as high as possible. Of course, one cannot make $\bar{F}_B = \bar{F}_C = 1$ due to no-cloning/broadcast theorems[33, 34]. The task is accomplished if one can make $\bar{F}_B$ and $\bar{F}_C$ as high as possible. In this sense the tripartite teleportation scheme is similar to a quantum copier (cloning device)[35, 36, 37, 38].

From the postulate of quantum mechanics on composite systems the state of the tripartite teleportation process should be

$$\rho_{in} \otimes \rho_{GHZ}. \tag{16}$$

As will be discussed below ρ_{GHZ} will be changed into $\varepsilon(\rho_{GHZ})$ if noise is introduced when Alice, Bob and Charlie prepare the GHZ state initially, where ε is a quantum operation[1].

After sharing GHZ state, Alice performs a projective measurement by preparing a set of the measurement operators $\{M_1, M_2, M_3, M_4\}$ with

$$M_1 = |\Phi^+\rangle\langle\Phi^+| \quad M_2 = |\Phi^-\rangle\langle\Phi^-| \quad M_3 = |\Psi^+\rangle\langle\Psi^+| \quad M_4 = |\Psi^-\rangle\langle\Psi^-|, \tag{17}$$

where

$$|\Phi^\pm\rangle = \frac{1}{\sqrt{2}}\left(|00\rangle \pm |11\rangle\right)_{12} \qquad |\Psi^\pm\rangle = \frac{1}{\sqrt{2}}\left(|01\rangle \pm |10\rangle\right)_{12}. \tag{18}$$

Since $|\Phi^{\pm}\rangle$ and $|\Psi^{\pm}\rangle$ form a Bell basis, the operators satisfy the completeness constraint

$$\sum_m M_m^{\dagger} M_m = I. \tag{19}$$

From the quantum mechanical postulates the probability P_m, probability that the result of the Alice's measurement is m, is given by

$$P_m = \mathrm{Tr}\left[\left(M_m^{\dagger} M_m \otimes I_{34}\right)\left(\rho_{in} \otimes \rho_{GHZ}\right)\right] \tag{20}$$

and the state of the system after the Alice's measurement reduces to

$$\tilde{\rho}_m = \frac{1}{P_m}(M_m \otimes I_{34})\left(\rho_{in} \otimes \rho_{GHZ}\right)(M_m \otimes I_{34})^{\dagger}. \tag{21}$$

For our case we have $P_1 = P_2 = P_3 = P_4 = 1/4$. After measurement, Alice broadcasts her measurement outcome to Bob and Charlie via a classical channel.

Next, let us consider the subsystem of Bob and Charlie. This process can be performed by tracing out the Alice's subsystem, *i.e*

$$\pi_{3,4}^m = \mathrm{Tr}_{1,2}\left(\tilde{\rho}_m\right). \tag{22}$$

Let us assume that the accomplice, Bob, performs a projective measurement again by preparing a set of measurement operators $\{N_1, N_2\}$ with

$$N_1 = |\mu^+\rangle\langle\mu^+| \qquad N_2 = |\mu^-\rangle\langle\mu^-|, \tag{23}$$

where

$$|\mu^+\rangle = \sin\nu|0\rangle + \cos\nu|1\rangle \qquad |\mu^-\rangle = \cos\nu|0\rangle - \sin\nu|1\rangle. \tag{24}$$

Since $|\mu^+\rangle$ and $|\mu^-\rangle$ form a basis for the Bob's qubit, the completeness condition

$$N_1^{\dagger} N_1 + N_2^{\dagger} N_2 = I \tag{25}$$

is naturally satisfied. From the quantum mechanical postulates again the probability q_{mn}, probability that the result of the Bob's measurement is n on condition that the outcome of Alice's measurement is m, reduces to

$$q_{mn} = \mathrm{Tr}\left[(N_n \otimes I_4)\pi_{3,4}^m\right] \tag{26}$$

and the state of the system after the Bob's measurement becomes

$$\tilde{\pi}_{mn} = \frac{1}{q_{mn}}(N_n \otimes I_4)\pi_{3,4}^m(N_n \otimes I_4)^{\dagger}. \tag{27}$$

For our case q_{mn} becomes

$$q_{11} = q_{21} = q_{32} = q_{42} = \frac{1}{2}\left(1 - \cos 2\nu\cos\theta\right) \qquad q_{12} = q_{22} = q_{31} = q_{41} = \frac{1}{2}\left(1 + \cos 2\nu\cos\theta\right). \tag{28}$$

Now, let us consider the subsystem of Charlie by tracing out the Bob's subsystem, *i.e.*

$$\chi_4^{mn} = \mathrm{Tr}_3\left(\tilde{\pi}_{mn}\right). \tag{29}$$

Finally, Charlie takes an appropriate unitary transformation to his own qubit

$$\tau_{mn} = u_4^{mn} \chi_4^{mn} \left(u_4^{mn}\right)^\dagger . \tag{30}$$

The unitary operator u_4^{mn} becomes

$$u_4^{11} = u_4^{22} = I \qquad u_4^{12} = u_4^{21} = \sigma_z \qquad u_4^{31} = u_4^{42} = \sigma_x \qquad u_4^{32} = u_4^{41} = \sigma_y \tag{31}$$

where σ_i is usual Pauli matrices. At this stage the tripartite teleportation process is terminated.

Now, we want to discuss the tripartite teleportation process through a noisy channel. If noise is introduced at the initial stage when Alice, Bob, and Charlie share their single qubit from $|GHZ\rangle$, ρ_{GHZ} is, in general, changed into the mixed state. The mixed state can be derived by solving a master equation in the Lindblad form[39]

$$\frac{\partial \rho}{\partial t} = -i[H_S, \rho] + \sum_{i,\alpha} \left(L_{i,\alpha} \rho L_{i,\alpha}^\dagger - \frac{1}{2} \left\{ L_{i,\alpha}^\dagger L_{i,\alpha}, \rho \right\} \right) \tag{32}$$

where the Lindblad operator $L_{i,\alpha} \equiv \sqrt{\kappa_{i,\alpha}} \sigma_\alpha^{(i)}$ acts on the ith qubit and describes decoherence. Of course, the operator $\sigma_\alpha^{(i)}$ denotes the Pauli matrix of the ith qubit with $\alpha = x, y, z$. The constant $\kappa_{i,\alpha}$ is approximately equal to the inverse of decoherence time. In this paper we will assume for simplicity that the constant $\kappa_{i,\alpha}$ is independent of i and α, *i.e.* $\kappa_{i,\alpha} = \kappa$.

Solutions of Eq.(32) for the $(L_{2,x}, L_{3,x}, L_{4,x})$, $(L_{2,y}, L_{3,y}, L_{4,y})$, $(L_{2,z}, L_{3,z}, L_{4,z})$ and isotropy noises were solved explicitly in Ref.[40]. The spectral decompositions of the results are as follows:

$$\begin{aligned}
\varepsilon_X(\rho_{GHZ}) &= x|GHZ,1\rangle\langle GHZ,1| + \frac{1-x}{3}\Big[|GHZ,3\rangle\langle GHZ,3| \\
&\quad + |GHZ,5\rangle\langle GHZ,5| + |GHZ,7\rangle\langle GHZ,7|\Big] \qquad \left(x = \frac{1}{4}(1+3e^{-4\kappa t})\right) \\
\varepsilon_Y(\rho_{GHZ}) &= \frac{y_+^3}{8}|GHZ,1\rangle\langle GHZ,1| + \frac{y_-^3}{8}|GHZ,2\rangle\langle GHZ,2| \\
&\quad + \frac{y_+ y_-^2}{8}\Big[|GHZ,3\rangle\langle GHZ,3| + |GHZ,5\rangle\langle GHZ,5| + |GHZ,7\rangle\langle GHZ,7|\Big] \\
&\quad + \frac{y_+^2 y_-}{8}\Big[|GHZ,4\rangle\langle GHZ,4| + |GHZ,6\rangle\langle GHZ,6| + |GHZ,8\rangle\langle GHZ,8|\Big] \\
&\qquad\qquad (y_\pm = 1 \pm e^{-2\kappa t}) \\
\varepsilon_Z(\rho_{GHZ}) &= z|GHZ,1\rangle\langle GHZ,1| + (1-z)|GHZ,2\rangle\langle GHZ,2| \qquad \left(z = \frac{1}{2}(1+e^{-6\kappa t})\right) \\
\varepsilon_I(\rho_{GHZ}) &= \frac{1+3p^2+4p^3}{8}|GHZ,1\rangle\langle GHZ,1| + \frac{1+3p^2-4p^3}{8}|GHZ,2\rangle\langle GHZ,2| \\
&\quad + \frac{1-p^2}{8}\Big[I - (|000\rangle\langle 000| + |111\rangle\langle 111|)\Big] \qquad (p = e^{-4\kappa t})
\end{aligned} \tag{33}$$

where the subscripts X, Y, Z, and I represent the type of noise channels, and

$$|GHZ,1\rangle = \frac{1}{\sqrt{2}}\left(|000\rangle + |111\rangle\right) \qquad |GHZ,2\rangle = \frac{1}{\sqrt{2}}\left(|000\rangle - |111\rangle\right) \tag{34}$$

$$|GHZ,3\rangle = \frac{1}{\sqrt{2}}\left(|001\rangle + |110\rangle\right) \qquad |GHZ,4\rangle = \frac{1}{\sqrt{2}}\left(|001\rangle - |110\rangle\right)$$
$$|GHZ,5\rangle = \frac{1}{\sqrt{2}}\left(|010\rangle + |101\rangle\right) \qquad |GHZ,6\rangle = \frac{1}{\sqrt{2}}\left(|010\rangle - |101\rangle\right)$$
$$|GHZ,7\rangle = \frac{1}{\sqrt{2}}\left(|011\rangle + |100\rangle\right) \qquad |GHZ,8\rangle = \frac{1}{\sqrt{2}}\left(|011\rangle - |100\rangle\right).$$

The probabilities P_m's and q_{mn}'s in the noisy channels can be directly computed by changing ρ_{GHZ} in Eq.(20) and Eq.(26) into the mixed states (33). The results for the $(L_{2,x}, L_{3,x}, L_{4,x})$, $(L_{2,y}, L_{3,y}, L_{4,y})$, $(L_{2,z}, L_{3,z}, L_{4,z})$[b], and isotropy noise channels are summarized in Table 1. As Table 1 indicates, P_m's and q_{mn}'s in the various noisy channels reduce to $P_i = 1/4 (i = 1, \cdots, 4)$ and Eq.(28) at $\kappa = 0$ limit.

Table 1. Basic Quantities in Tripartite Teleportation

quantities	no noise and Z noise	X and Y noises	Isotropy noise
P_1, P_2, P_3, P_4	$\frac{1}{4}$	$\frac{1}{4}$	$\frac{1}{4}$
$q_{11}, q_{21}, q_{32}, q_{42}$	$\frac{1}{2}(1 - \cos 2\nu \cos\theta)$	$\frac{1}{2}(1 - \cos 2\nu \cos\theta e^{-4\kappa t})$	$\frac{1}{2}(1 - \cos 2\nu \cos\theta e^{-8\kappa t})$
$q_{31}, q_{41}, q_{12}, q_{22}$	$\frac{1}{2}(1 + \cos 2\nu \cos\theta)$	$\frac{1}{2}(1 + \cos 2\nu \cos\theta e^{-4\kappa t})$	$\frac{1}{2}(1 + \cos 2\nu \cos\theta e^{-8\kappa t})$

3. Fidelities

The fidelity, which measures how well the initial state ρ_{in} is transported to Charlie's final state, can be computed as follows. Since Charlie's final state is τ_{mn} provided that Alice and Bob measure m and n respectively, one can define the fidelity F^C_{mn} in this case as a form

$$F^C_{mn} = \mathrm{Tr}\left[\tau_{mn}\rho_{in}\right]. \tag{35}$$

Averaging over all possible measurement outcomes, we can define the average fidelity with fixed ρ_{in} in a form

$$F_C(\theta,\phi) = \sum_{m=1}^{4}\sum_{n=1}^{2} P_m q_{mn} F^C_{mn}. \tag{36}$$

Finally, averaging $F_C(\theta,\phi)$ over all possible input states, we can define the average fidelity $\bar{F}_C$ for all possible ρ_{in} as follows:

$$\bar{F}_C = \frac{1}{4\pi}\int_0^{\pi} d\theta \int_0^{2\pi} d\phi \sin\theta F_C(\theta,\phi). \tag{37}$$

When there is no noise, $F_C(\theta,\phi)$ and $\bar{F}_C$ becomes

$$F_C(\theta,\phi) = 1 - \frac{1}{2}(1 - \sin 2\nu)\sin^2\theta \qquad \bar{F}_C = \frac{1}{3}(2 + \sin 2\nu). \tag{38}$$

Thus, the fidelities between Alice and Charlie depend on the set of Bob's measurement operators. If Bob chooses $\nu = \pi/4$, $\bar{F}_C$ reaches to its maximum $\bar{F}_C = 1$, which means the perfect teleportation from Alice to Charlie.

[b]For notational simplicity, we will use the terminology X-, Y-, and Z-noises together for $(L_{2,x}, L_{3,x}, L_{4,x})$, $(L_{2,y}, L_{3,y}, L_{4,y})$, $(L_{2,z}, L_{3,z}, L_{4,z})$ noises

The fidelities $F_C(\theta,\phi)$ and $\bar{F}_C$ are summarized in Table 2 when the mixed states changed from $|GHZ\rangle$ by various noises are introduced as a quantum channel. Comparing Table 2 with Table I of Ref.[40], one can realize that $F_C(\theta,\phi)$ and $\bar{F}_C$ with $\nu=\pi/4$ exactly coincide with fidelities of the bipartite teleportation when same noises are introduced initially in the quantum channel.

Table 2. Fidelities between ρ_{in} and Charlie's final state τ_{mn}

Type of noise	$F_C(\theta,\phi)$	F_C
no noise	$1-\frac{1}{2}(1-\sin 2\nu)\sin^2\theta$	$\frac{1}{3}(2+\sin 2\nu)$
X noise	$\frac{1}{2}[(1+\sin^2\theta\cos^2\phi\sin 2\nu)$ $+e^{-4\kappa t}(\cos^2\theta+\sin^2\theta\sin^2\phi\sin 2\nu)]$	$\frac{1}{6}[(3+\sin 2\nu)$ $+e^{-4\kappa t}(1+\sin 2\nu)]$
Y noise	$\frac{1}{2}[1+e^{-2\kappa t}\sin^2\theta\sin^2\phi\sin 2\nu+e^{-4\kappa t}\cos^2\theta$ $+e^{-6\kappa t}\sin^2\theta\cos^2\phi\sin 2\nu]$	$\frac{1}{6}[3+e^{-2\kappa t}\sin 2\nu$ $+e^{-4\kappa t}+e^{-6\kappa t}\sin 2\nu]$
Z noise	$1-\frac{1}{2}(1-\sin 2\nu e^{-6\kappa t})\sin^2\theta$	$\frac{1}{3}[2+e^{-6\kappa t}\sin 2\nu]$
Isotropy noise	$\frac{1}{2}[1+e^{-8\kappa t}\cos^2\theta+e^{-12\kappa t}\sin^2\theta\sin 2\nu]$	$\frac{1}{6}[3+e^{-8\kappa t}+2\sin 2\nu e^{-12\kappa t}]$

In the tripartite teleportation scheme, however, there are additional fidelities between Alice's state ρ_{in} and Bob's final state. Since Bob's final state after his measurement is N_1 or N_2 defined in Eq.(23) with respective probability $\sum_{i=1}^{4}P_iq_{i1}$ or $\sum_{i=1}^{4}P_iq_{i2}$, the average fidelities between ρ_{in} and Bob's final state can be defined as

$$F_B^T(\theta,\phi)=\mathrm{Tr}[N_1\rho_{in}]\sum_{i=1}^{4}P_iq_{i1}+\mathrm{Tr}[N_2\rho_{in}]\sum_{i=1}^{4}P_iq_{i2} \tag{39}$$
$$\bar{F}_B^T=\frac{1}{4\pi}\int_0^{\pi}d\theta\int_0^{2\pi}d\phi\sin\theta F_B^T(\theta,\phi).$$

If one computes $F_B^T(\theta,\phi)$ and $\bar{F}_B^T$ for X-, Y-, Z-, and isotropy-noise channels, one can show that they are all same as

$$F_B^T(\theta,\phi)=\bar{F}_B^T=\frac{1}{2}. \tag{40}$$

This is too small because the optimal value for a classical teleportation scheme is 2/3.

However, one can define fidelities at the stage just after Alice broadcasts her measurement outcome to Bob and Charlie via classical channel. If Alice's outcome is m, then the fidelities between ρ_{in} and Bob's final state can be defined as

$$F_B^m(\theta,\phi)=q_{m1}\mathrm{Tr}[N_1\rho_{in}]+q_{m2}\mathrm{Tr}[N_2\rho_{in}] \tag{41}$$
$$\bar{F}_B^m=\frac{1}{4\pi}\int_0^{\pi}d\theta\int_0^{2\pi}d\phi\sin\theta F_B^m(\theta,\phi).$$

When there is no noise, it is straightforward to show that $F_B^m(\theta,\phi)$ and $\bar{F}_B^m$ become

$$F_B^{m=1}(\theta,\phi)=F_B^{m=2}(\theta,\phi)=\frac{1}{2}\left[1+\cos^2 2\nu\cos^2\theta-\sin 2\nu\cos 2\nu\sin\theta\cos\theta\cos\phi\right] \tag{42}$$
$$F_B^{m=3}(\theta,\phi)=F_B^{m=4}(\theta,\phi)=\frac{1}{2}\left[1-\cos^2 2\nu\cos^2\theta+\sin 2\nu\cos 2\nu\sin\theta\cos\theta\cos\phi\right]$$
$$\bar{F}_B^{m=1}=\bar{F}_B^{m=2}=\frac{2}{3}-\frac{1}{6}\sin^2 2\nu$$
$$\bar{F}_B^{m=3}=\bar{F}_B^{m=4}=\frac{1}{3}+\frac{1}{6}\sin^2 2\nu.$$

When $m = 1$ or 2, $\bar{F}_B^m$ reaches to its maximum value 2/3 if $\nu = 0$ and $\nu = \pi/2$. At the same time fidelity $\bar{F}_C$ becomes its minimum value 2/3. When $\bar{F}_B^m$ reaches to its minimum value 1/2 at $\nu = \pi/4$, $\bar{F}_C$ becomes its maximum value 1. Thus, one can increase/decrease $\bar{F}_B^m$ at the cost of decreasing/increasing $\bar{F}_C$.

Table 3. Fidelities between ρ_{in} and Bob's state just after Alice broadcasts her outcome.

Type of noise	Alice's outcome	$F_B^m(\theta,\phi)$	$\bar{F}_B^m$
X-noise and Y-noise	$m = 1,2$	$\frac{1}{2} + \frac{1}{2}\cos 2\nu \cos 2\theta \times (\cos 2\nu \cos\theta - \sin 2\nu \sin\theta)\, e^{-4\kappa t}$	$\frac{1}{6}\left(3 + e^{-4\kappa t}\cos^2 2\nu\right)$
	$m = 3,4$	$\frac{1}{2} - \frac{1}{2}\cos 2\nu \cos 2\theta \times (\cos 2\nu \cos\theta - \sin 2\nu \sin\theta)\, e^{-4\kappa t}$	$\frac{1}{6}\left(3 - e^{-4\kappa t}\cos^2 2\nu\right)$
no-noise and Z-noise	$m = 1,2$	$\frac{1}{2}\Big(1 + \cos^2 2\nu \cos^2\theta - \sin 2\nu \cos 2\nu \sin\theta \cos\theta \cos\phi\Big)$	$\frac{2}{3} - \frac{1}{6}\sin^2 2\nu$
	$m = 3,4$	$\frac{1}{2}\Big(1 - \cos^2 2\nu \cos^2\theta + \sin 2\nu \cos 2\nu \sin\theta \cos\theta \cos\phi\Big)$	$\frac{1}{3} + \frac{1}{6}\sin^2 2\nu$
Isotropy noise	$m = 1,2$	$\frac{1}{2} + \frac{1}{2}\cos 2\nu \cos 2\theta \times (\cos 2\nu \cos\theta - \sin 2\nu \sin\theta)\, e^{-8\kappa t}$	$\frac{1}{6}\left(3 + e^{-8\kappa t}\cos^2 2\nu\right)$
	$m = 3,4$	$\frac{1}{2} - \frac{1}{2}\cos 2\nu \cos 2\theta \times (\cos 2\nu \cos\theta - \sin 2\nu \sin\theta)\, e^{-8\kappa t}$	$\frac{1}{6}\left(3 - e^{-8\kappa t}\cos^2 2\nu\right)$

The fidelities $F_B^m(\theta,\phi)$ and $\bar{F}_B^m$ are summarized in Table 3 when the various noisy channels are introduced. One of the interesting points of Table 3 is that the fidelities for the Z-noisy channel are independent of the noise parameter κ while $F_C(\theta,\phi)$ and $\bar{F}_C$ are dependent on κ as Table II indicated. The ν- and κt-dependence of $\bar{F}_C$ and $\bar{F}_B^m(m = 1,2)$ in $(L_{2,z}, L_{3,z}, L_{4,z})$ noisy channel is plotted together in Fig. 1. The upper surface in the figure corresponds to $\bar{F}_C$ and the lower one to $\bar{F}_B^m$. The difference between $\bar{F}_C$ and $\bar{F}_B^m$ is averagely maximized when $\kappa = 0$, which means there is no noise. If, however, κt becomes larger and larger, the difference between two fidelities becomes negligible. This is due to the fact that the effect of noise is significant compared to the choice of ν in the Bob's measurement. One can find a similar behaviors in the other noisy channels although we have not presented the ν- and κt-dependence of the fidelities explicitly in this paper.

4. π-tangle

In this section we will compute the π-tangle of the various noisy channels defined in Eq.(12). When there is no noise, it is easy to show that

$$||\rho_{GHZ}^{T_A}|| = ||\rho_{GHZ}^{T_B}|| = ||\rho_{GHZ}^{T_C}|| = 2, \tag{43}$$

which results in

$$\mathcal{N}_{A(BC)} = \mathcal{N}_{B(AC)} = \mathcal{N}_{C(AB)} = 1. \tag{44}$$

In addition, one can show that there is no contribution to the entanglement from the two-

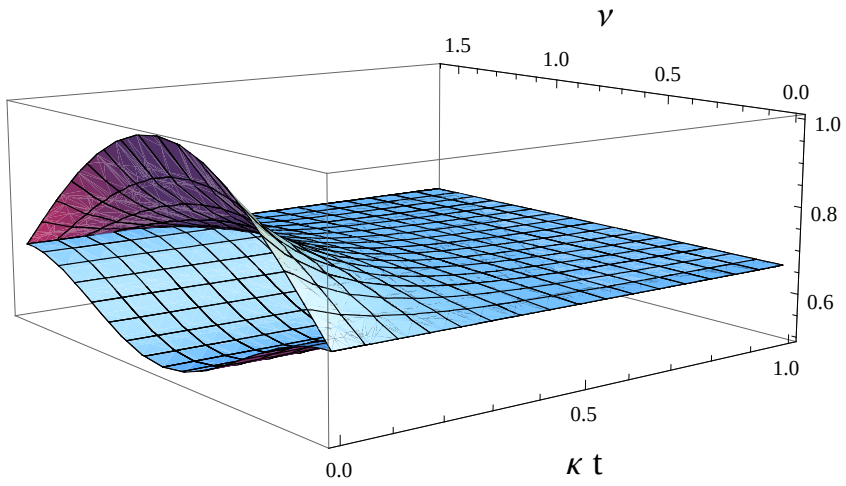

Fig. 1. The ν- and κt-dependence of $\bar{F}_C$ and $\bar{F}_B^m$ with $m = 1, 2$ when the type of noise is $(L_{2,z}, L_{3,z}, L_{4,z})$. The upper and lower surfaces correspond to $\bar{F}_C$ and $\bar{F}_B^m$ respectively. The difference between $\bar{F}_C$ and $\bar{F}_B^m$ is maximized in the $\kappa t \to 0$ limit. However, this difference becomes negligible with increasing κt. This is due to the fact that decoherence is a major dominant effect in the region of large κt.

tangles in GHZ state:

$$\mathcal{N}_{AB} = \mathcal{N}_{AC} = \mathcal{N}_{BC} = 0. \tag{45}$$

Thus, π-tangle for the GHZ state is simply

$$\pi_{ABC}^{GHZ} = 1, \tag{46}$$

which indicates that the GHZ state is a maximally entangled state.

The π-tangles for $(L_{2,x}, L_{3,x}, L_{4,x})$, $(L_{2,y}, L_{3,y}, L_{4,y})$, $(L_{2,z}, L_{3,z}, L_{4,z})$, and isotropy channels can be computed straightforwardly. For all noisy channels $\mathcal{N}_{A(BC)} = \mathcal{N}_{B(AC)} = \mathcal{N}_{C(AB)}$ and $\mathcal{N}_{AB} = \mathcal{N}_{AC} = \mathcal{N}_{BC} = 0$ hold. This seems to be due to the fact that we have considered only same-axis noisy channels. The π-tangles for the various noisy channels are summarized at Table 4. The interesting fact Table 4 indicates is that while the π-tangles for the X- and Z-noise channels vanish at $\kappa t \to \infty$ limit, those for the Y- and isotropy-noise channels goes to zero when $y_* \leq \kappa t \leq \infty$ and $i_* \leq \kappa t \leq \infty$ respectively, where

$$\begin{aligned} y_* &= \ln \frac{1 + (19 + 3\sqrt{33})^{1/3} + (19 - 3\sqrt{33})^{1/3}}{3} \sim 0.609378 \\ i_* &= \frac{1}{4} \ln \frac{(54 + 3\sqrt{321})^{1/3} + (54 - 3\sqrt{321})^{1/3}}{3} \sim 0.146435. \end{aligned} \tag{47}$$

Table 4. The π-tangles for the various noisy channels.

Type of noise	π-tangle
no noise	1
X noise	$e^{-8\kappa t}$
Y noise	$\frac{1}{64}\Big[\lvert 1-3e^{-2\kappa t}-e^{-4\kappa t}-e^{-6\kappa t}\rvert -(1-3e^{-2\kappa t}-e^{-4\kappa t}-e^{-6\kappa t})\Big]^2$
Z noise	$e^{-12\kappa t}$
Isotropy noise	$\frac{1}{64}\Big[\lvert 1-e^{-8\kappa t}-4e^{-12\kappa t}\rvert -(1-e^{-8\kappa t}-4e^{-12\kappa t})\Big]^2$

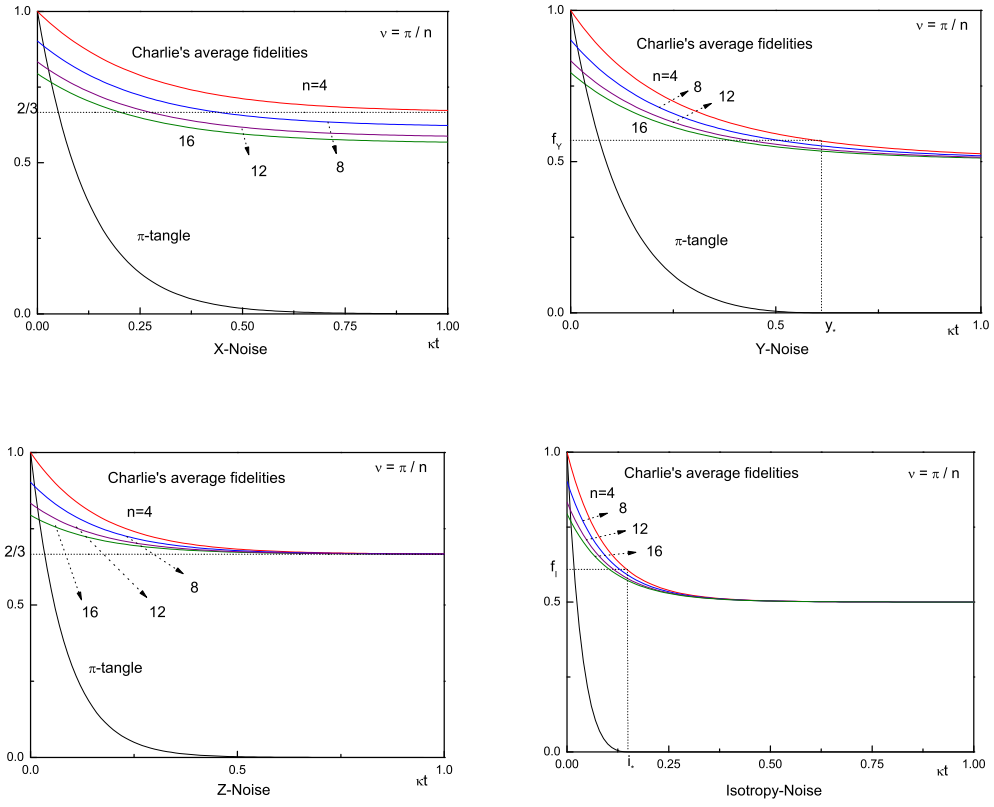

Fig. 2. The κt dependence of π-tangles and average fidelities $\bar{F}_C$ in $(L_{2,x}, L_{3,x}, L_{4,x})$ (Fig. 2a), $(L_{2,y}, L_{3,y}, L_{4,y})$ (Fig. 2b), $(L_{2,z}, L_{3,z}, L_{4,z})$ (Fig. 2c), and isotropy (Fig. 2d) noisy channels.

The κt-dependence of π-tangles together with average fidelity $\bar{F}_C$ for the various noisy channels are plotted in Fig. 2. In the Z-noisy channel the π-tangle vanishes at $\kappa t = \infty$ and

at this limit $\bar{F}_C$ goes to 2/3 regardless of ν, which is a classical fidelity limit. In the X-noise channel $\bar{F}_C$ goes to $(3+\sin 2\nu)/6$ at $\kappa t = \infty$. When $\nu = \pi/4$, this also goes to 2/3. Therefore, the π-tangles for X- and Z-noise channels seem to show a nice connection between $\bar{F}_C$ and tripartite entanglement of the given channel.

However, this nice property is not maintained in the Y- and isotropy-noise channel. In the Y-noise channel the π-tangle vanishes at $y_* \leq \kappa t$. At $\kappa t = y_*$ $\bar{F}_C$ reduces to $0.166667(3.08738+ 0.321426\sin 2\nu)$, whose maximum is $f_Y = 0.568314$. Thus f_Y is much less than the classical fidelity limit 2/3. Similar behavior can be found in the isotropy channel. In this channel the π-tangle vanishes at $i_* \leq \kappa t$. At $\kappa t = i_*$ the maximum of fidelity $\bar{F}_C$ becomes $f_I = 0.609159$, which is also less than the classical limit 2/3.

5. three-tangle

In this section we would like to discuss the three-tangles for the various noisy channels expressed in Eq.(33).

5.1. $(L_{2,z}, L_{3,z}, L_{4,z})$ *noisy channel*

Let us consider the pure state

$$|Z(z,\varphi)\rangle = \sqrt{z}|GHZ,1\rangle - e^{i\varphi}\sqrt{1-z}|GHZ,2\rangle \tag{48}$$

where $z = (1+e^{-6\kappa t})/2$. It is easy to show that the three-tangle of $|Z(z,\varphi)\rangle$ is

$$\tau_3\left(|Z(z,\varphi)\rangle\right) = (1-2z+2z^2) - 2z(1-z)\cos 2\varphi. \tag{49}$$

Thus, $\tau_3\left(|Z(z,\varphi)\rangle\right)$ has a minimum at $\varphi = 0$ and $\varphi = \pi$, i.e.

$$\tau_3\left(|Z(z,0)\rangle\right) = \tau_3\left(|Z(z,\pi)\rangle\right) = (1-2z)^2. \tag{50}$$

In terms of the terminologies of Ref.[41] $(1-2z)^2$ forms a convex characteristic curve in $(z, \tau_3\left(|Z(z,\varphi)\rangle\right))$ plane. In addition, one can show straightforwardly that $\varepsilon(\rho_{GHZ})$ defined in Eq.(33) can be decomposed into

$$\varepsilon(\rho_{GHZ}) = \frac{1}{2}|Z(z,0)\rangle\langle Z(z,0)| + \frac{1}{2}|Z(z,\pi)\rangle\langle Z(z,\pi)|. \tag{51}$$

If Eq.(51) is optimal, then the three-tangle for $\varepsilon(\rho_{GHZ})$ is $(2z-1)^2$. Since this coincides with the convex characteristic curve, Eq.(51) should be the optimal decomposition. Thus, the three-tangle for the $\varepsilon(\rho_{GHZ})$ is

$$\tau^z_{ABC} = (1-2z)^2 = e^{-12\kappa t}. \tag{52}$$

It is interesting to note that the three-tangle and π-tangle are the same with each other in this channel.

5.2. $(L_{2,x}, L_{3,x}, L_{4,x})$ *noisy channel*

Before we start computation, it is worthwhile noting that as shown in Ref.[23] the state

$$\Pi_{GHZ} = \frac{1}{3}\Big[|GHZ,3\rangle\langle GHZ,3| + |GHZ,5\rangle\langle GHZ,5| + |GHZ,7\rangle\langle GHZ,7|\Big] \tag{53}$$

has vanishing three-tangle. This fact is shown in appendix A.

Now, let us consider a pure state

$$|X(x,\varphi_1,\varphi_2,\varphi_3)\rangle = \sqrt{x}|GHZ,1\rangle - e^{i\varphi_1}\sqrt{\frac{1-x}{3}}|GHZ,3\rangle \\ -e^{i\varphi_2}\sqrt{\frac{1-x}{3}}|GHZ,5\rangle - e^{i\varphi_3}\sqrt{\frac{1-x}{3}}|GHZ,7\rangle \tag{54}$$

where $x = (1+3e^{-4\kappa t})/4$. Then it is easy to show that the three-tangle of $|X(x,\varphi_1,\varphi_2,\varphi_3)\rangle$ becomes

$$\begin{aligned}&\tau_3\left(|X(x,\varphi_1,\varphi_2,\varphi_3)\rangle\right) \\ &= \Bigg| x^2 + \frac{(1-x)^2}{9}\left(e^{4i\varphi_1}+e^{4i\varphi_2}+e^{4i\varphi_3}\right) - \frac{2}{3}x(1-x)\left(e^{2i\varphi_1}+e^{2i\varphi_2}+e^{2i\varphi_3}\right) \\ &\quad -\frac{2}{9}(1-x)^2\left(e^{2i(\varphi_1+\varphi_2)}+e^{2i(\varphi_1+\varphi_3)}+e^{2i(\varphi_2+\varphi_3)}\right) - \frac{8\sqrt{3}}{9}\sqrt{x(1-x)^3}e^{i(\varphi_1+\varphi_2+\varphi_3)}\Bigg|.\end{aligned} \tag{55}$$

The vectors $|X(x,\varphi_1,\varphi_2,\varphi_3)\rangle$ has following properties. The three-tangle of it has the largest zero at $x = x_0 \equiv 3/4$ and $\varphi_1 = \varphi_2 = \varphi_3 = 0$. The vectors $|X(x,0,0,0)\rangle$, $|X(x,0,\pi,\pi)\rangle$, $|X(x,\pi,0,\pi)\rangle$ and $|X(x,\pi,\pi,0)\rangle$ have same three-tangles. Finally, $\varepsilon_X(\rho_{GHZ})$ can be decomposed into

$$\varepsilon_X(\rho_{GHZ}) = \frac{1}{4}\Big[|X(x,0,0,0)\rangle\langle X(x,0,0,0)| + |X(x,0,\pi,\pi)\rangle\langle X(x,0,\pi,\pi)| \\ +|X(x,\pi,0,\pi)\rangle\langle X(x,\pi,0,\pi)| + |X(x,\pi,\pi,0)\rangle\langle X(x,\pi,\pi,0)|\Big]. \tag{56}$$

When $x \le x_0$, one can construct the optimal decomposition in the following form:

$$\varepsilon_X(\rho_{GHZ}) = \frac{x}{4x_0}\Big[|X(x_0,0,0,0)\rangle\langle X(x_0,0,0,0)| + |X(x_0,0,\pi,\pi)\rangle\langle X(x_0,0,\pi,\pi)| \\ +|X(x_0,\pi,0,\pi)\rangle\langle X(x_0,\pi,0,\pi)| + |X(x_0,\pi,\pi,0)\rangle\langle X(x_0,\pi,\pi,0)|\Big] \\ +\frac{x_0-x}{x_0}\Pi_{GHZ}. \tag{57}$$

Since Π_{GHZ} has vanishing three-tangle, one can show easily

$$\tau^X_{ABC} = 0 \qquad \text{when} \quad x \le x_0 = 3/4. \tag{58}$$

Now, let us consider the three-tangle of $\varepsilon_X(\rho_{GHZ})$ in the region $x_0 \le x \le 1$. Since Eq.(56) is an optimal decomposition at $x = x_0$, one can conjecture that it is also optimal in the region $x_0 \le x$. As will be shown shortly, however, this is not true at the large-x region. If we compute the three-tangle under the condition that Eq.(56) is optimal at $x_0 \le x$, its expression becomes

$$\alpha^X_I(x) = x^2 - \frac{1}{3}(1-x)^2 - 2x(1-x) - \frac{8\sqrt{3}}{9}\sqrt{x(1-x)^3}. \tag{59}$$

However, one can show straightforwardly that $\alpha_I^X(x)$ is not a convex function in the region $x \geq x_*$, where

$$x_* = \frac{1}{4}\left(1 + 2^{1/3} + 4^{1/3}\right) \approx 0.961831. \tag{60}$$

Therefore, we need to convexify $\alpha_I^X(x)$ in the region $x_1 \leq x \leq 1$ to make the three-tangle to be convex function, where x_1 is some number between x_0 and x_*. The number x_1 will be determined shortly.

In the large x-region one can derive the optimal decomposition in a form:

$$\begin{aligned}
&\varepsilon_X(\rho_{GHZ}) \qquad (61)\\
&= \frac{1-x}{4(1-x_1)}\Big[|X(x_1,0,0,0)\rangle\langle X(x_1,0,0,0)| + |X(x_1,0,\pi,\pi)\rangle\langle X(x_1,0,\pi,\pi)| \\
&\qquad +|X(x_1,\pi,0,\pi)\rangle\langle X(x_1,\pi,0,\pi)| + |X(x_1,\pi,\pi,0)\rangle\langle X(x_1,\pi,\pi,0)|\Big] \\
&\qquad +\frac{x-x_1}{1-x_1}|GHZ,1\rangle\langle GHZ,1|
\end{aligned}$$

which gives a three-tangle as

$$\alpha_{II}^X(x,x_1) = \frac{1-x}{1-x_1}\alpha_I^X(x_1) + \frac{x-x_1}{1-x_1}. \tag{62}$$

Since $d^2\alpha_{II}^X/dx^2 = 0$, there is no convex problem if $\alpha_{II}^X(x,x_1)$ is a three-tangle in the large-x region. The constant x_1 can be fixed from the condition of minimum α_{II}^X, i.e. $\partial\alpha_{II}^X(x,x_1)/\partial x_1 = 0$, which gives

$$x_1 = \frac{1}{4}(2+\sqrt{3}) \approx 0.933013. \tag{63}$$

As expected x_1 is between x_0 and x_*. Thus, finally the three-tangle for $\varepsilon_X(\rho_{GHZ})$ becomes

$$\tau_{ABC}^X = \begin{cases} 0 & x \leq x_0 \\ \alpha_I^X(x) & x_0 \leq x \leq x_1 \\ \alpha_{II}^X(x,x_1) & x_1 \leq x \leq 1 \end{cases} \tag{64}$$

and the corresponding optimal decompositions are Eq.(57), Eq.(56) and Eq.(61) respectively. In terms of κt τ_{ABC}^X reduces to

$$\tau_{ABC}^X = \begin{cases} \alpha_{II}^X(x,x_1) & 0 \leq \kappa t \leq \mu_1^X \\ \alpha_I^X(x) & \mu_1^X \leq \kappa t \leq \mu_2^X \\ 0 & \mu_2^X \leq \kappa t \leq \infty \end{cases} \tag{65}$$

where $x = (1+3e^{-4\kappa t})/3$ and

$$\mu_1^X = -\frac{1}{4}\ln\frac{4x_1-1}{3} \approx 0.0233899 \qquad \mu_2^X = -\frac{1}{4}\ln\frac{2}{3} \approx 0.101366. \tag{66}$$

5.3. $(L_{2,y}, L_{3,y}, L_{4,y})$ *noisy channel*

The mixed state $\varepsilon_Y(\rho_{GHZ})$ given in Eq.(33) can be re-written as

$$\varepsilon_Y(\rho_{GHZ}) = \xi \Pi_1^{GHZ}(Y_1) + (1-\xi)\Pi_2^{GHZ}(Y_2) \tag{67}$$

where

$$\begin{aligned}\Pi_1^{GHZ}(Y_1) &= Y_1|GHZ,1\rangle\langle GHZ,1| \\ &\quad + \frac{1-Y_1}{3}\Big[|GHZ,3\rangle\langle GHZ,3| + |GHZ,5\rangle\langle GHZ,5| + |GHZ,7\rangle\langle GHZ,7|\Big] \\ \Pi_2^{GHZ}(Y_2) &= Y_2|GHZ,2\rangle\langle GHZ,2| \\ &\quad + \frac{1-Y_2}{3}\Big[|GHZ,4\rangle\langle GHZ,4| + |GHZ,6\rangle\langle GHZ,6| + |GHZ,8\rangle\langle GHZ,8|\Big].\end{aligned} \tag{68}$$

In Eq.(68) the constants are given by

$$\xi = \frac{y_+(y_+^2+3y_-^2)}{8} \qquad Y_1 = \frac{y_+^2}{y_+^2+3y_-^2} \qquad Y_2 = \frac{y_-^2}{3y_+^2+y_-^2} \tag{69}$$

where $y_\pm = 1 \pm e^{-2\kappa t}$. It is worthwhile noting that $\Pi_2^{GHZ}(Y_2)$ is local-unitary (LU) equivalent to $\Pi_1^{GHZ}(Y_2)$, i.e.

$$\Pi_1^{GHZ}(Y_2) = (\sigma_z \otimes I \otimes I)\Pi_2^{GHZ}(Y_2)(\sigma_z \otimes I \otimes I)^\dagger.$$

Since the three-tangle is LU-invariant quantity, the three-tangle for $\Pi_2^{GHZ}(Y_2)$ should be equal to that for $\Pi_1^{GHZ}(Y_2)$. From a fact that $\Pi_1^{GHZ}(Y_2)$ can be obtained from $\varepsilon_X(\rho_{GHZ})$ by replacing x by Y_2, one can compute the three-tangle for $\Pi_2^{GHZ}(Y_2)$ directly from Eq.(64). Since, furthermore, $Y_2 \leq 1/4$ in the entire range of κt, the three-tangle for $\Pi_2^{GHZ}(Y_2)$ should be zero.

The state $\varepsilon_Y(\rho_{GHZ})$ is rank-8 mixed state and it seems to be highly difficult to compute the three-tangle analytically. So far, in fact, there is no general method for the computation of the three-tangle for the rank-8 mixed states. However, one can compute its upper bound as following. Since the three-tangle for $\Pi_2^{GHZ}(Y_2)$ is zero and the three-tangle for the mixed state is obtained by the convex-roof method, Eq.(67) implies that the three-tangle for $\varepsilon_Y(\rho_{GHZ})$ should be less than ξ times three-tangle for $\Pi_1^{GHZ}(Y_1)$. Since $\Pi_1^{GHZ}(Y_1)$ is same with $\varepsilon_X(\rho_{GHZ})$ if x is replaced by Y_1, one can compute the upper bound of the three-tangle for $\varepsilon_Y(\rho_{GHZ})$, $\tau_{ABC}^{Y:UB}$ directly from Eq.(64). The superscript UB stands for upper bound. The final result of this upper bound can be summarized as

$$\tau_{ABC}^{Y:UB} = \begin{cases} \xi\alpha_{II}^X(Y_1,x_1) & 0 \leq \kappa t \leq \nu_1^* \\ \xi\alpha_I^X(Y_1) & \nu_1^* \leq \kappa t \leq \nu_2^* \\ 0 & \nu_2^* \leq \kappa t \leq \infty \end{cases} \tag{70}$$

where

$$\nu_1^* = -\frac{1}{2}\ln(\sqrt{3}-1) \sim 0.155953 \qquad \nu_2^* = \frac{1}{2}\ln 2 \sim 0.346574. \tag{71}$$

Of course, x_1 is given in Eq.(63).

Although we have derived the non-trivial upper bound of three-tangle for $\varepsilon_Y(\rho_{GHZ})$, it is worthwhile noting that Eq.(70) does not have any information on the real three-tangle for

the rank-8 mixed state $\varepsilon_Y(\rho_{GHZ})$ because it is derived from a particular decomposition (67). The only one we know is that Eq.(70) is larger than the real three-tangle derived from the optimal decomposition.

5.4. *isotropy noisy channel*

The mixed state $\varepsilon_I(\rho_{GHZ})$ given in Eq.(33) can be re-written as

$$\varepsilon_I(\rho_{GHZ}) = \zeta\Sigma_1^{GHZ} + (1-\zeta)\Sigma_2^{GHZ} \tag{72}$$

where

$$\begin{aligned}\Sigma_1^{GHZ} &= \left(\frac{1}{2} + \frac{2p^3}{1+3p^2}\right)|GHZ,1\rangle\langle GHZ,1| \\ &\quad + \left(\frac{1}{2} - \frac{2p^3}{1+3p^2}\right)|GHZ,2\rangle\langle GHZ,2| \\ \Sigma_2^{GHZ} &= \frac{1}{6}\left\{I - (|000\rangle\langle 000| + |111\rangle\langle 111|)\right\}\end{aligned} \tag{73}$$

and

$$\zeta = \frac{1+3p^2}{4} \tag{74}$$

with $p = e^{-4\kappa t}$.

The state $\varepsilon_I(\rho_{GHZ})$ is rank-8 mixed state and we do not know how to compute the three-tangle of it exactly. Since, however, the three-tangle of Σ_2^{GHZ} is zero, one can compute at least the upper bound as ζ times three-tangle of Σ_1^{GHZ}. This upper bound can be easily computed by making use of the analytical result of the three-tangle for the Z-noise channel. The final result of this upper bound is

$$\tau_{ABC}^{I:UB} = \frac{4p^6}{1+3p^2} = \frac{4e^{-24\kappa t}}{1+3e^{-8\kappa t}} \tag{75}$$

where the superscript UB stands for the upper bound. As stressed before, Eq.(75) does not have any relation to the real three-tangle of $\varepsilon_I(\rho_{GHZ})$. It is merely a quantity which is larger than the real three-tangle of the rank-8 mixed state $\varepsilon_I(\rho_{GHZ})$.

6. Conclusion

In this paper we have computed the π-tangles explicitly for the mixed states summarized in Eq.(33). It is shown that the π-tangles for the X- and Z-noisy channels vanish at $\kappa t \to \infty$, where the maximum of $\bar{F}_C$ reduces to the classical limit 2/3. However, this nice property is not maintained for the Y- and isotropy-noise channels. For Y-noise the π-tangle vanishes at $y_* \leq \kappa t$, where y_* is given by Eq.(47). At $\kappa t = y_*$ the maximum $\bar{F}_C$ becomes 0.57, which is much less than the classical limit. For isotropy noise the π-tangle vanishes when $i_* \leq \kappa t$. At $\kappa t = i_*$ the maximum $\bar{F}_C$ becomes 0.61, which is also less than the classical limit. Although the π-tangle was constructed in Ref.[24] to reflect the tripartite entanglement of the W-type states, it does not seem to give a meaningful interpretation in real quantum information processes.

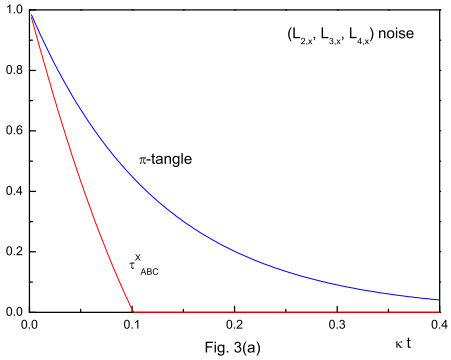

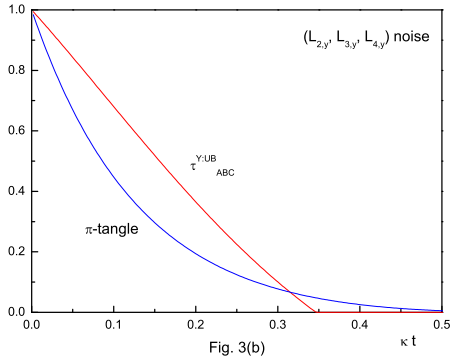

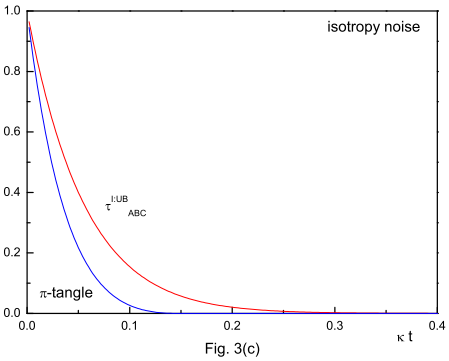

Fig. 3. The κt dependence of the three-tangle and π-tangle for the $(L_{2,x}, L_{3,x}, L_{4,x})$ (Fig. 3a), $(L_{2,y}, L_{3,y}, L_{4,y})$ (Fig. 3b), and isotropy (Fig. 3c) noisy channels.

We have also computed the three-tangles for the X- and Z-noise channels. The remarkable fact is that the three-tangle for the Z-noise channel is exactly the same with the corresponding π-tangle. Therefore, the three-tangle for the Z-noise channel vanishes at $\kappa t \rightarrow \infty$, where all $\bar{F}_C$ reduce to the classical limit regardless of Bob's measurement outcome. For X-noise the κt-dependence of the three tangle is plotted in Fig. 3(a). For comparison we plot the corresponding π-tangle together. As Fig. 3(a) shows, the three-tangle is much less than the corresponding π-tangle. In this channel the three-tangle vanishes when $\mu_2^X \leq \kappa t$, where $\mu_2^X = -(1/4)\ln(2/3)$. At $\kappa t = \mu_2^X$ the fidelity $\bar{F}_C$ becomes $(11 + 5\sin 2\nu)/18$. When, therefore, $\nu = (1/2)\sin^{-1}(1/5) \sim 0.100679$, $\bar{F}_C$ reduces to the classical limit $2/3$. However, the maximum fidelity goes to $8/9$, which is much larger than that of the classical limit.

The κt-dependence of $\tau_{ABC}^{Y:UB}$ and $\tau_{ABC}^{I:UB}$ are plotted in Fig. 3(b) and Fig. 3(c) respectively. For comparison we plot the corresponding π-tangle together. Fig. 3(b) shows that $\tau_{ABC}^{Y:UB}$ is larger than the corresponding π-tangle when $0 \leq \kappa t \leq 0.315$. Fig. 3(c) shows that $\tau_{ABC}^{I:UB}$ is larger than the corresponding π-tangle in the entire range of κt. This is due to the fact that $\tau_{ABC}^{Y:UB}$ and $\tau_{ABC}^{I:UB}$ are merely the upper bounds of the real three-tangles for the Y- and

isotropy-noise channels. If the calculational tool for the three-tangle of arbitrary three-party mixed states are developed someday, probably the real three-tangles computed via this tool are less than the corresponding π-tangles.

In this paper we have examined the physical meaning of the three-tangle and π-tangle in the real quantum information process. We adopted the tripartite teleportation via various noisy channels as a model of quantum process. It is shown that the π-tangle seems to be too large to have a meaningful interpretation. Although we cannot compute the three-tangles for the Y- and isotropy-noise channels due to their high rank, the results for X- and Z-noise seems to imply the fact that the three-tangle is too small to have meaningful interpretation. Probably, we need a different tripartite entanglement measure whose value is between three-tangle and π-tangle.

Acknowledgements

This work was supported by the Kyungnam University Foundation Grant, 2008.

References

1. M. A. Nielsen and I. L. Chuang, *Quantum Computation and Quantum Information* (Cambridge University Press, Cambridge, England, 2000).
2. C. H. Bennett, G. Brassard, C. Crépeau, R. Jozsa, A. Peres and W. K. Wootters, *Teleporting an Unknown Quantum State via Dual Classical and Einstein-Podolsky-Rosen Channles*, Phys. Rev. Lett. **70** (1993) 1895.
3. C. H. Bennett and S. J. Wiesner, *Communication vi one- and two-particle operators on Einstein-Podolsky-Rosen states*, Phys. Rev. Lett. **69** (1992) 2881.
4. G. Vidal, *Efficient classical simulation of slightly entangled quantum computations*, Phys. Rev. Lett. **91** (2003) 147902 [quant-ph/0301063].
5. T. C. Wei and P. M. Goldbart, *Geometric measure of entanglement and applications to bipartite and multipartite quantum states*, Phys. Rev. **A68** (2003) 042307 [quant-ph/0307219]; H. Barnum, E. Knill, G. Ortiz, R. Somma, and L. Viola, *A Subsystem-Independent Generalization of Entanglement*, Phys. Rev. Lett. **92**, 107902 (2004) [quant-ph/0305023]; L. Aolita and F. Mintert, *Measuring Multipartite Concurrence with a Single Factorizable Observable*, Phys. Rev. Lett. **97**, 050501 (2006); Y. Most, Y. Shimoni, and O. Biham, *Formation of multipartite entanglement using random quantum gates*, Phys. Rev. A **76**, 022328 (2007) [quant-ph/0708.3481]; C. E. López, G. Romero, F. Lastra, E. Solano, and J. C. Retamal, *Sudden Birth versus Sudden Death of Entanglement in Multipartite Systems*, Phys. Rev. Lett. **101**, 080503 (2008) [quant-ph/0802.1825]; L. Tamaryan, D. K. Park and S. Tamaryan, *Analytic Expressions for Geometric Measure of Three Qubit States*, Phys. Rev. **A 77** (2008) 022325, [quant-ph/0710.0571].
6. C. H. Bennett, D. P. DiVincenzo, J. A. Smokin and W. K. Wootters, *Mixed-state entanglement and quantum error correction*, Phys. Rev. **A54** (1996) 3824 [quant-ph/9604024].
7. A. Uhlmann, *Fidelity and concurrence of conjugate states*, Phys. Rev. **A 62** (2000) 032307 [quant-ph/9909060].
8. S. Hill and W. K. Wootters, *Entanglement of a Pair of Quantum Bits*, Phys. Rev. Lett. **78** (1997) 5022 [quant-ph/9703041].
9. W. K. Wootters, *Entanglement of Formation of an Arbitrary State of Two Qubits*, Phys. Rev. Lett. **80** (1998) 2245 [quant-ph/9709029].
10. V. Coffman, J. Kundu and W. K. Wootters, *Distributed entanglement*, Phys. Rev. **A61** (2000) 052306 [quant-ph/9907047].

11. A. Cayley, *On the Theory of Linear Transformations*, Cambridge Math. J. **4** (1845) 193.
12. A. Miyake, *Classification of multipartite entangled states by multidimensional determinants*, Phys. Rev. **A67** (2003) 012108 [quant-ph/0206111].
13. F. Verstraete, J. Dehaene and B. D. Moor, *Normal forms and entanglement measures for multipartite quantum states*, Phys. Rev. **A68** (2003) 012103 [quant-ph/0105090].
14. M. S. Leifer, N. Linden and A. Winter, *Measuring polynomial invariants of multiparty quantum states*, Phys. Rev. **A69** (2004) 052304 [quant-ph/0308008].
15. W. Dür, G. Vidal, and J. I. Cirac, *Three qubits can be entangled in two inequivalent ways*, Phys. Rev. **A62** (2000) 062314 [quant-ph/0005115].
16. D. M. Greenberger, M. Horne, and A. Zeilinger, *Bell's Theorem, Quantum Theory, and Conceptions of the Universe*, edited by M. Kafatos (Kluwer, Dordrecht, 1989) p 69.
17. N. Linden, S. Popescu, and W. K. Wootters, *Almost Every Pure State of Three Qubits Is Completely Determined by Its Two-Particle Reduced Density Matrices*, Phys. Rev. Lett. **89**, 207901 (2002) [quant-ph/0207109]; S. N. Walck and D. W. Lyons, *Only n-Qubit Greenberger-Horne-Zeilinger States Are Undetermined by Their Reduced Density Matrices*, Phys. Rev. Lett. **100**, 050501 (2008) arXiv: 0808.0859 (quant-ph).
18. P. Parashar and S. Rana, *N-Qubit W States are Determined by their Bipartite Marginals*, Phys. Rev. A **80**, 012319 (2009); 0809.4394 (quant-ph).
19. S. Tamaryan, T.-C. Wei, and D.K. Park, *Maximally entangled three-qubit states via geometric measure of entanglement*, Phys. Rev. A **80**, (2009) 052315, arXiv: 0905.3791v4 [quant-ph].
20. R. Lohmayer, A. Osterloh, J. Siewert and A. Uhlmann, *Entangled Three-Qubit States without Concurrence and Three-Tangle*, Phys. Rev. Lett. **97** (2006) 260502 [quant-ph/0606071].
21. C. Eltschka, A. Osterloh, J. Siewert and A. Uhlmann, *Three-tangle for mixtures of generalized GHZ and generalized W states*, New J. Phys. **10** (2008) 043014, arXiv:0711.4477 (quant-ph).
22. E. Jung, M. R. Hwang, D. K. Park and J. W. Son, *Three-tangle for Rank-3 Mixed States: Mixture of Greenberger-Horne-Zeilinger, W and flipped W states*, Phys. Rev. **A79** (2009) 024306, arXiv:0810.5403 (quant-ph).
23. E. Jung, D. K. Park, and J. W. Son, *Three-tangle does not properly quantify tripartite entanglement for Greenberger-Horne-Zeilinger-type state*, Phys. Rev. **A80** 010301(R), arXiv:0901.2610 (quant-ph).
24. Y. U. Ou and H. Fan, *Monogamy Inequality in terms of Negativity for Three-Qubit States*, Phys. Rev. **A75** (2007) 062308 [quant-ph/0702127].
25. G. Vidal and R. F. Werner, *Computable measure of entanglement*, Phys. Rev. **A65** (2002) 032314 [quant-ph/0102117].
26. A. Peres, *Separability Criterion for Density Matrices*, Phys. Rev. Lett. **77** (1996) 1413 [quant-ph/9604005].
27. M. Horodecki, P. Horodecki and R. Horodecki, *Separability of mixed states: necessary and sufficient conditions*, Phys. Lett. **A 223** (1996) 1 [quant-ph/9605038].
28. P. Horodecki, *Separability criterion and inseparable mixed states with partial transposition*, Phys. Lett. **A 232** (1997) 333 [quant-ph/9703004]
29. A. Karlsson and M. Bourennane, *Quantum teleportation using three-particle entanglement*, Phys. Rev. **A58** (1998) 4394.
30. E. Jung, M. R. Hwang, D. K. Park, J. W. Son and S. Tamaryan, *Mixed-state entanglement and quantum teleportation through noisy channels*, J. Phys. A: Math. Theor. **41** (2008) 385302 [arXiv:0804.4595 (quant-ph)].
31. S. Popescu, *Bell's Inequalities versus Teleportation: What is Nonlocality*, Phys. Rev. Lett. **72** (1994) 797.
32. Y. Yeo, *Quantum teleportation using three-particle entanglement*, quant-ph/0302030.
33. W. K. Wootters and W. H. Zurek, *A single quantum cannot be cloned*, Nature, **299** (1982) 802.
34. H. Barnum, C. M. Caves, C. A. Fuchs, R. Jozsa and B. Schumacher, *Noncommuting Mixed States Cannot Be Broadcast*, Phys. Rev. Lett. **76** (1996) 2818 [quant-ph/9511010].
35. V. Buzek and M. Hillery, *Quantum copying: Beyond the no-cloning theorem*, Phys. Rev. **A54**

(1996) 1844 [quant-ph/9607018].
36. V. Buzek, V. Vedral, M. B. Plenio, P. L. Knight, and M. Hillery, *Broadcasting of entanglement via local copying*, Phys. Rev. **A55** (1997) 3327 [quant-ph/9701028].
37. V. Buzek, S. L. Braunstein, M. Hillery, and D. Bruss, *Quantum copying: A network*, Phys. Rev. **A56** (1997) 3446 [quant-ph/9703046].
38. N. Gisin and S. Massar, *Optimal Quantum Cloning Machines*, Phys. Rev. Lett. **79** (1997) 2153 [quant-ph/9705046].
39. G. Lindblad, *On the generators of quantum dynamical semigroups*, Commun. Math. Phys. **48** (1976) 119.
40. Eylee Jung, Mi-Ra Hwang, You-Hwan Ju, Min-Soo Kim, Sahng-Kyoon Yoo, Hungsoo Kim, DaeKil Park, Jin-Woo Son, S. Tamaryan, and Seong-Keuck Cha, *Greenberger-Horne-Zeilinger versus W: Quantum Teleportation through Noisy Channels*, Phys. Rev. **A78** (2008) 012312 [arXiv:0801.1433 (quant-ph)].
41. A. Osterloh, J. Siewert and A. Uhlmann, *Tangles of superpositions and the convex-roof extension*, Phys. Rev. **A77** (2008) 032310, arXiv:0710.5909 (quant-ph).

Appendix A

In this appendix we would like to prove that Π_{GHZ} defined in Eq.(53) has vanishing three-tangle. Consider a pure state

$$|J(\theta_1,\theta_2)\rangle = \frac{1}{\sqrt{3}}|GHZ,3\rangle - \frac{1}{\sqrt{3}}e^{i\theta_1}|GHZ,5\rangle - \frac{1}{\sqrt{3}}e^{i\theta_2}|GHZ,7\rangle. \tag{A.1}$$

Then, it is easy to show that the three-tangle of $|J(\theta_1,\theta_2)\rangle$ is

$$\tau_3(\theta_1,\theta_2) = \frac{1}{9}|1-\left(e^{i\theta_1}-e^{i\theta_2}\right)^2||1-\left(e^{i\theta_1}+e^{i\theta_2}\right)^2|, \tag{A.2}$$

which vanishes when

$$\begin{aligned}
&(i) \quad e^{i\theta_1}-e^{i\theta_2}=1 \Longrightarrow (\theta_1=\pi/3,\theta_2=2\pi/3),(\theta_1=5\pi/3,\theta_2=4\pi/3) \\
&(ii) \quad e^{i\theta_1}-e^{i\theta_2}=-1 \Longrightarrow (\theta_1=2\pi/3,\theta_2=\pi/3),(\theta_1=4\pi/3,\theta_2=5\pi/3) \\
&(iii) \quad e^{i\theta_1}+e^{i\theta_2}=1 \Longrightarrow (\theta_1=\pi/3,\theta_2=5\pi/3),(\theta_1=5\pi/3,\theta_2=\pi/3) \\
&(iv) \quad e^{i\theta_1}+e^{i\theta_2}=-1 \Longrightarrow (\theta_1=2\pi/3,\theta_2=4\pi/3),(\theta_1=4\pi/3,\theta_2=2\pi/3).
\end{aligned} \tag{A.3}$$

Furthermore, one can show straightforwardly that Π_{GHZ} can be decomposed into

$$\begin{aligned}
\Pi_{GHZ} = \frac{1}{8}\Bigg[& |J\left(\frac{\pi}{3},\frac{2\pi}{3}\right)\rangle\langle J\left(\frac{\pi}{3},\frac{2\pi}{3}\right)| + |J\left(\frac{\pi}{3},\frac{5\pi}{3}\right)\rangle\langle J\left(\frac{\pi}{3},\frac{5\pi}{3}\right)| \\
& + |J\left(\frac{2\pi}{3},\frac{\pi}{3}\right)\rangle\langle J\left(\frac{2\pi}{3},\frac{\pi}{3}\right)| + |J\left(\frac{2\pi}{3},\frac{4\pi}{3}\right)\rangle\langle J\left(\frac{2\pi}{3},\frac{4\pi}{3}\right)| \\
& + |J\left(\frac{4\pi}{3},\frac{2\pi}{3}\right)\rangle\langle J\left(\frac{4\pi}{3},\frac{2\pi}{3}\right)| + |J\left(\frac{4\pi}{3},\frac{5\pi}{3}\right)\rangle\langle J\left(\frac{4\pi}{3},\frac{5\pi}{3}\right)| \\
& + |J\left(\frac{5\pi}{3},\frac{\pi}{3}\right)\rangle\langle J\left(\frac{5\pi}{3},\frac{\pi}{3}\right)| + |J\left(\frac{5\pi}{3},\frac{4\pi}{3}\right)\rangle\langle J\left(\frac{5\pi}{3},\frac{4\pi}{3}\right)| \Bigg].
\end{aligned} \tag{A.4}$$

Combining Eq.(A.3) and (A.4), one can show that Eq.(A.4) is the optimal decomposition of Π_{GHZ} and the three-tangle is

$$\tau_3\left(\Pi_{GHZ}\right) = 0. \tag{A.5}$$